Available online at www.sciencedirect.com
SCIENCE DIRECT®
Journal of Nuclear Materials 337–339 (2005) 276–280
journal of nuclear materials
www.elsevier.com/locate/jnucmat

Effect of drifts on the high Mach flow associated with the divertor detachment

K. Hoshino [a], A. Hatayama [a,*], R. Schneider [b], D.P. Coster [c]

[a] *Department of Applied Physics and Physico-informatics, Faculty of Science and Technology, Keio University, 3-14-1 Hiyoshi, Kouhoku-ku, Yokohama-shi 223-0061, Japan*
[b] *Max-Planck-Institut für Plasmaphysik, Greifswald, Germany*
[c] *Max-Planck-Institut für Plasmaphysik, Garching, Germany*

Abstract

Effects of drifts have been studied on high Mach flows near the *X*-point associated with the divertor plasma detachment. Numerical calculations using a 2D edge plasma simulation code (the B2.5-EIRENE code) have been made for the JT-60U W-shaped divertor geometry. In this article, we mainly focus our attention to the effect of $\mathbf{E}\times\mathbf{B}$ drift. The cases with and without $\mathbf{E}\times\mathbf{B}$ drift in the partial detached state are compared. Due to the strong decrease of electron temperature near the separatrix and the resultant radial electric field, poloidal $\mathbf{E}\times\mathbf{B}$ drift flows are observed in the simulation. But the radial profiles of basic plasma parameters are not so much affected. In addition, simple model has been applied to discuss the numerical results. Although the drifts possibly act as a parallel momentum source/sink, the effect on the parallel flows is shown to be relatively small.

PACS: 52.55.Fa; 52.40.Hf; 52.65.−y
Keywords: B2.5-Eirene code; Detachment; JT-60U; Drift effects

1. Introduction

High parallel flows associated with plasma detachment have been observed in several tokamak experiments [1,2]. Large Mach flows up to Mach 1 or even larger have been measured near the *X*-point away from the target plate in these experiments (Henceforth, abbreviation 'HMAD' will be used for such high Mach flows associated with the detachment state). Recently, a numerical simulation using B2-EIRENE code [3–5] has been done to clarify the physical mechanism of HMAD [6]. In addition, comparison of numerical results with experiments in JT-60U has been done, and the effects of divertor geometry on HMAD were also studied [7]. Qualitative features of the radial profile of HMAD obtained by the 2D simulations agree well with those by the experiments, and divertor geometry has strong effects on the radial structure of HMAD. However, in these analyses [6,7], the effects of drifts and current are not taken into account. These effects possibly affect the HMAD and the flow structure in the detached state in the divertor region. The purpose of this study is to clarify the effects of various drifts on HMAD. In this article, we focus our main attention to the $\mathbf{E}\times\mathbf{B}$ drift on HMAD.

* Corresponding author. Tel.: +81 45 566 1607; fax: +81 45 566 1587.
E-mail addresses: ouzak@ppl.appi.keio.ac.jp (K. Hoshino), akh@ppl.appi.keio.ac.jp (A. Hatayama).

0022-3115/$ - see front matter © 2004 Elsevier B.V. All rights reserved.
doi:10.1016/j.jnucmat.2004.10.039

2. B2.5-EIRENE simulation

2.1. Numerical model

In order to take into account the effects of various drifts and also currents in the edge plasma, the B2.5-EIRENE code package [8] has been applied to the analysis of JT-60U W-shaped plasmas. In the analysis, neutral behavior has been simulated by kinetic neutral transport code (EIRENE code [4,9]) instead of a simple neutral fluid model, since the neutral transport has an important role especially in the detachment plasma.

Fig. 1 shows the numerical mesh generated from JT-60U MHD equilibrium of shot #029623. This shot is a typical of the large volume, L mode discharges for JT-60U. The basic plasma parameters of this shot are as follows: the plasma current $I_p = 1.2\,\mathrm{MA}$, the toroidal magnetic field $B_t = 3.5\,\mathrm{T}$, and the effective safety factor $q_{eff} = 4.4$.

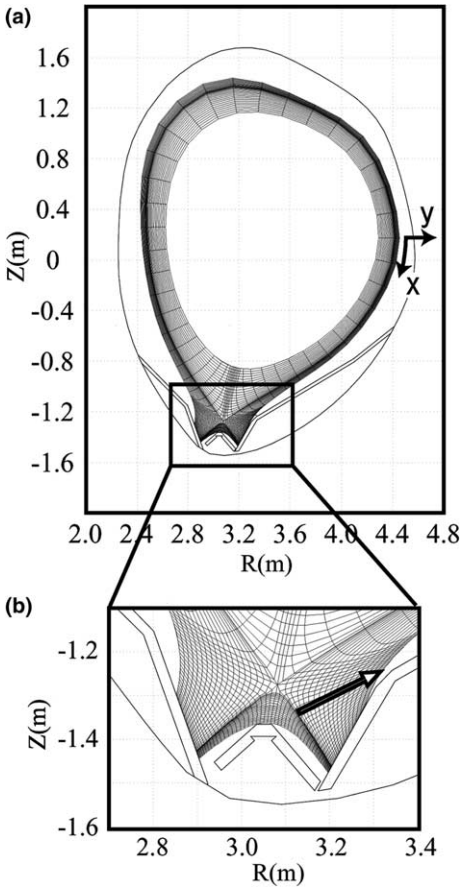

Fig. 1. The JT-60U geometrical configuration. (a) Numerical grids for the analysis and the vacuum vessel and (b) zoom-in view of the divertor region.

At the core interface boundary, bulk ion density and the input power are fixed to be $n_D = 3.2 \times 10^{19}\,\mathrm{m}^{-3}$ and $Q_{in} = 2.5\,\mathrm{MW}$, respectively. The remaining conditions are the same as those in Refs. [6,7].

2.2. Simulation results

In Fig. 2(a), negative electric field is observed close to the separatrix near the X-point (along arrow in Fig. 1). This is caused by the local decrease of electron temperature associated with the partial detachment. This tendency agrees well with experimental result [10] as shown in Fig. 2(c). Particle flux density by $\mathbf{E}\times\mathbf{B}$ drift due to this electric field is shown in Fig. 2(b). The amount of the poloidal flux due to the $\mathbf{E}\times\mathbf{B}$ drift becomes about 30% of the poloidal projection of the parallel particle flux $nv_{\parallel}$. The direction is toward upstream from the target plate as in the experimental result in Fig. 2(d). Qualitatively these tendencies agree well with the experiment.

In Fig. 3, the simulation results of the basic parameters, such as (a) electron density, (b) electron temperature and (c) parallel Mach number, are plotted along the arrow shown in Fig. 1. The circles and squares show the results for the case without and with $\mathbf{E}\times\mathbf{B}$ drift, respectively. The effect of $\mathbf{E}\times\mathbf{B}$ drift on the radial profiles of basic plasma parameters near the X-point is very small. In both cases, electron temperature T_e near the separatrix is less than 5 eV and this region becomes in the partial detached state. As shown in Fig. 3(c), in this detached region, the HMAD can be seen, i.e., the parallel Mach number increases up to about $M \sim 0.8$. As was discussed in Refs. [6,7], the driving mechanism of this HMAD is explained as follows: (1) the decrease in T_e toward the target plate along the field line leads to the clear separation of the ionization region near the X-point and the momentum loss region in front of the target plate. (2) static pressure drops in the ionization region mainly due to the rapid T_e decrease along the field line, while the total (static and dynamic) pressure is being kept almost constant, and (3) dynamic pressure $mnv_{\parallel}^2$ increases due to (1) and (2). Outside the partial detachment region, T_e is relatively high and the outer region is still in the attachment state. The Mach number in this region is relatively low $M \sim 0.2$.

3. Simple model considerations

To understand simulation results, we discuss the effects of drifts on parallel momentum balance by a simple model. The simple model is basically the same as that in Refs. [11,12]. The effect of diamagnetic drift is also included. We use the coordinate system shown in Fig. 1 for the (x,y)-plane and Fig. 4 for the (x,z)-plane.

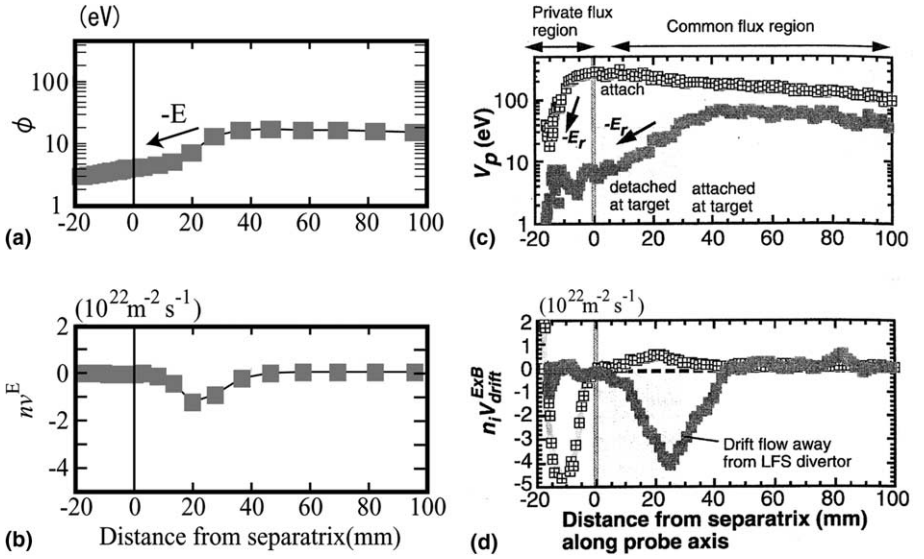

Fig. 2. The simulation results of (a) potential and (b) particle flux density due to the $\mathbf{E}\times\mathbf{B}$ drift, are plotted along arrow shown in Fig. 1. The experimental profile of (c) potential and (d) particle flux density under attached (closed square) and detached (open square with cross) divertor condition are measured by reciprocating Mach probe, which scans from private flux region to low field side (LFS) divertor plate just below the X-point. The arrow shown in Fig. 1 almost corresponds to scanning path of reciprocating Mach probe.

3.1. Basic equations

The steady-state continuity equation and momentum equation are given by

$$\nabla\cdot(n\mathbf{v}_{i,e}) = S^{p}, \tag{1}$$

$$m_{i,e}n(\mathbf{v}_{i,e}\cdot\nabla)\mathbf{v}_{i,e} = -\nabla P_{i,e} \pm en(\mathbf{E}+\mathbf{v}_{i,e}\times\mathbf{B}) - m_{i,e}\mathbf{v}_{i,e}S^{p} + \mathbf{S}^{m}, \tag{2}$$

where $m_{i,e}$ are masses, $P_{i,e}$ are pressure, $\mathbf{E}$ is electric field, $\mathbf{v}_{i,e}$ are fluid velocities, n is number density (we assume $n\sim n_i\sim n_e$). Subscript i and e correspond to ion and electron, respectively. The particle source from ionization is denoted S^{p}, and $\mathbf{S}^{m}$ is the momentum sink by collision with neutrals. The drift velocity in the radial direction is derived from Eq. (2) as follows [11].

$$v_y = v_y^{E} + v_y^{D},$$
$$\text{where } v_y^{E} = -\cos\theta\frac{E_x}{B},\ v_y^{D} = \cos\theta\frac{1}{enB}\frac{\partial P}{\partial x}, \tag{3}$$

where v_y^{E} and v_y^{D} are the $\mathbf{E}\times\mathbf{B}$ drift and the diamagnetic drift velocity, respectively. Here, we have used the relation $P_i\sim P_e\sim P/2$ by assuming $T_i\sim T_e$. Though T_i is slightly higher than T_e in the simulation result, the assumption is almost valid. The electric field E_x can be estimated from electron parallel momentum equation as $E_x\sim-(1/2en)(\partial P/\partial x)$.

On the other hand, for the perpendicular drift velocity, more precisely, for the velocity perpendicular both to the magnetic field and the radial direction, we have

$$v_\perp = v_\perp^{E} + v_\perp^{D},\quad \text{where } v_\perp^{E} = \frac{E_y}{B},\ v_\perp^{D} = -\frac{1}{enB}\frac{P}{\partial y}. \tag{4}$$

Here, we assume that the radial electric field $E_y = -\partial\phi/\partial y\sim-(\partial/\partial y)(kT_e/e)$ near the separatrix. The simulation results in Section 2.2 support this assumption.

From Eqs. (1)–(4), we can obtain the following parallel momentum equation,

$$\frac{\partial}{\partial x}\left(mnv_\parallel^2 + P\right) = S^{E} + S^{D} + S^{m}, \tag{5}$$

where

$$S^{E,D} = \frac{\partial}{\partial y}\left(\frac{mnv_\parallel v_y^{E,D}}{\sin\theta}\right) + \frac{\partial}{\partial x}\left(\frac{mnv_\parallel v_\perp^{E,D}}{\tan\theta}\right), \tag{6}$$

are the momentum sources/sinks due to the $\mathbf{E}\times\mathbf{B}$ drift and the diamagnetic drift.

3.2. Effects of drifts on parallel momentum balance

In order to discuss the effects of drifts on the HMAD, we compare the momentum source/sink term $S^{E,D}$ due to the drifts in Eq. (6) with the driving force of the HMAD, i.e., the pressure gradient $-\partial P/\partial x$ near the X-point. From Eq. (6), the ratios of the momentum source/sink terms $S^{E,D}$ to $-\partial P/\partial x$ are estimated to be,

$$C^{E} = -\frac{mv_\parallel}{2eB\tan\theta}\left(\frac{1}{\lambda_P^y}+\frac{1}{\lambda_v^y}\right) - \frac{mv_\parallel\lambda_P^x}{2eB\lambda_T^x\tan\theta}\left(\frac{1}{\lambda_v^x}-\frac{1}{\lambda_P^x}\right), \tag{7}$$

$$C^{D} = 2C^{E}, \tag{8}$$

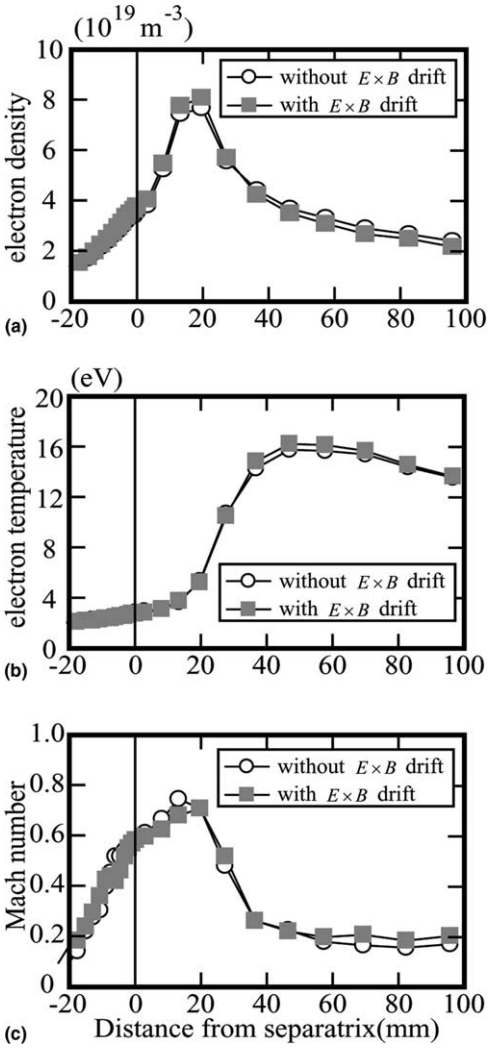

Fig. 3. The radial profiles of the basic plasma parameters are plotted along the arrow shown in Fig. 1: (a) electron density, (b) electron temperature and (c) parallel Mach number.

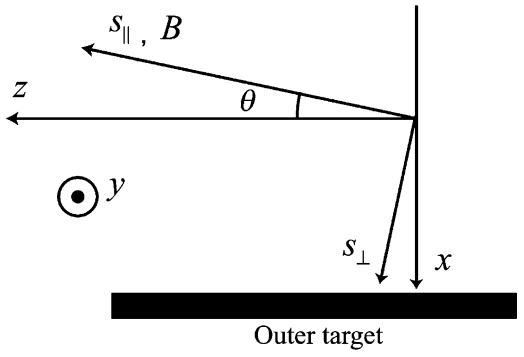

Fig. 4. The coordinate system used in the simple model.

where $\lambda_P^j, \lambda_v^j, \lambda_T^j$ $(j = x, y)$ are the characteristic decay length of pressure, parallel velocity and electron temperature in the jth direction, respectively. Here, we have used the relation $\partial P/\partial x \sim -P/\lambda_P^x$ due to the negative pressure gradient toward the divertor. The first term and the second term in the RHS of Eq. (7) correspond to the effect of the radial drift and the poloidal drift, respectively.

From the simulation results close to the separatrix near the X-point, i.e., inside the partial detachment region, the parameters in Eq. (7) are roughly estimated as, $v_\parallel \approx 10^4$ m/s, $B \approx 3.4$ T, $\theta \approx 0.02$ rad, and λ_P^j, λ_v^j, λ_T^j $(j = x, y)$ is larger than at least a few centimeters. Then, $|C^E| \approx 0.08$ and the effect of the $\mathbf{E}\times\mathbf{B}$ drift on parallel momentum is very small. Whether the S^E plays a role as the parallel momentum *source* or *sink* depends on the direction of the gradient of the basic plasma parameters. Near the separatrix, $C^E < 0$ and S^E becomes the parallel momentum *sink*. In fact, close to the separatrix, the Mach number slightly decreases with the effect of the $\mathbf{E}\times\mathbf{B}$ drift in the numerical simulation.

On the other hand, outside the detached region, i.e., far from the separatrix, S^E becomes momentum *source*, because the gradients of the basic parameters are reversed as seen from Fig. 3. The Mach number in this region becomes slightly larger with the $\mathbf{E}\times\mathbf{B}$ drift than without $\mathbf{E}\times\mathbf{B}$ drift in the simulation. However, the effect is also small.

From Eq. (8), the effect of diamagnetic drift on the parallel momentum balance is estimated to be at most two times larger than that by the $\mathbf{E}\times\mathbf{B}$ drift. Therefore, the effect is also negligible on HMAD, at least, by the present simple model without grad-B and Pfirsch-Schlüter effect.

4. Summary and future study

To investigate the effects of the $\mathbf{E}\times\mathbf{B}$ drift on the HMAD near the X-point, the B2.5-EIRENE simulation has been done. Due to the strong radial decrease of T_e near the separatrix associated with the partial detachment and the resultant electric field, large particle flux by the $\mathbf{E}\times\mathbf{B}$ drift toward the upstream near the X-point is observed as in the experiment in Ref. [10]. But, the effect of the $\mathbf{E}\times\mathbf{B}$ drift on the HMAD is shown to be small. The HMAD ($M \sim 0.8$) is driven mainly by the pressure gradient force along the field line due to the partial detachment near the separatrix away from the plates. To examine these simulation results, the effects of drifts on the parallel momentum balance were estimated also by the simple model. Although drifts possibly act as parallel momentum source or sink near the X-point, the effect on the HMAD is shown to be small as in the numerical results.

The Mach number outside the partial detached region away from the separatrix, still remains low and M becomes at most $M \sim 0.2$ in the numerical simulation. However, in the experiment in Ref. [10], relatively high Mach flows with $M \sim 0.5$ are also observed in the attached region. The numerical results presented here cannot reproduce such tendency. The physical mechanism, which drives relatively high Mach flow in the attached region, is still an open question. The possible causes are suggested by Refs. [10,13]. One of the possible causes is the effect of ∇B drift and Pfirsch-Schlüter flow, which is not taken into account in the present analysis. As has been pointed out in Ref. [10], Pfirsch-Schlüter effect possibly drives the relatively high Mach flow at mid-plane SOL, where the relatively large ∇T_i exists. This relatively high Mach flow at the mid-plane SOL possibly affects the flow near the X-point. Simulations with these effects are now underway.

Acknowledgments

The authors (K.H. and A.H.) gratefully acknowledge to Dr N. Asakura (JAERI) for his variable discussions.

References

[1] N. Tsois et al., J. Nucl. Mater. 266–269 (1999) 1230.
[2] N. Asakura et al., Nucl. Fus. 39 (1999) 1983.
[3] B.J. Braams et al., Fus. Technol. 9 (1986) 320.
[4] D. Reiter et al., Plasma Phys. Control. Fus. 33 (1991) 1579.
[5] R. Schneider et al., J. Nucl. Mater. 196–198 (1992) 810.
[6] A. Hatayama et al., Nucl. Fus. 40 (2000) 2009.
[7] A. Hatayama et al., High Mach flow associated with plasma detachment in JT-60U, in: Proceedings of the 19th IAEA Fusion Energy Conference, Lyon, France, October 2002.
[8] D.P. Coster et al., Further developments of the edge transport simulation package, SOLPS, in: Proceedings of the 19th IAEA Fusion Energy Conference, Lyon, France, October 2002.
[9] D. Reiter et al., J. Nucl. Mater. 196–198 (1992) 80.
[10] N. Asakura et al., J. Nucl. Mater. 313 (2003) 820.
[11] T.D. Rognlien, D.D. Ryutov, Contrib. Plasma Phys. 152–157 (1998) 38.
[12] P.C. Stangeby, A.V. Chankin, Nucl. Fus. 36 (1996) 839.
[13] G. Kirnev et al., Edge code simulations of SOL flows in JET, in: Proceedings of 16th PSI, Portland Maine, USA, May 2004.